CASE FILE
COPY

N 62 54382

NACA TN 2382

NATIONAL ADVISORY COMMITTEE FOR AERONAUTICS

TECHNICAL NOTE 2382

EFFECT OF HORIZONTAL-TAIL SIZE AND TAIL LENGTH ON LOW-SPEED STATIC LONGITUDINAL STABILITY AND DAMPING IN PITCH OF A MODEL HAVING 45° SWEPTBACK WING AND TAIL SURFACES

By Jacob H. Lichtenstein

Langley Aeronautical Laboratory
Langley Field, Va.

Washington
June 1951

NATIONAL ADVISORY COMMITTEE FOR AERONAUTICS

TECHNICAL NOTE 2382

EFFECT OF HORIZONTAL-TAIL SIZE AND TAIL LENGTH ON LOW-SPEED STATIC LONGITUDINAL STABILITY AND DAMPING IN PITCH OF A MODEL HAVING 45° SWEPTBACK WING AND TAIL SURFACES

By Jacob H. Lichtenstein

SUMMARY

An investigation has been conducted in the Langley stability tunnel to determine the effects of horizontal tails of various sizes and at various tail lengths when located at the center line of the fuselage on the low-speed static longitudinal stability and the steady-state rotary damping in pitch of a complete model with wing and tail surfaces having the quarter-chord lines swept back 45° and aspect ratios of 4.

The results of the investigation show that, in agreement with analytical considerations, the contribution of the horizontal tail to static longitudinal stability is directly related to the tail size and length; whereas the contribution to the rotary damping in pitch is directly related to the tail size and square of the tail length.

For low angles of attack the downwash of the wing reduced the effectiveness of the tail in contributing static longitudinal stability by approximately one-half; whereas the wing had practically no effect on the effectiveness of the tail in contributing to the rotary damping in pitch. For the tail positions investigated herein, the static longitudinal stability was slightly greater near the stall than at an angle of attack of 0°; whereas the damping in pitch was somewhat less near the stall than at an angle of attack of 0°.

At an angle of attack of about 10°, the static longitudinal stability of the wing-fuselage combinations changed adversely. The magnitude of this change was slightly increased by the addition of tail area at the shortest tail length but was decreased by addition of tail area at the longest tail length.

INTRODUCTION

Requirements for satisfactory high-speed performance of aircraft have resulted in configurations that differ in many respects from previous designs. As a result of these changes, the designer has little assurance that the low-speed characteristics will be satisfactory for any specific configuration. The low-speed characteristics of wings, suitable for high-speed flight, have already been investigated quite extensively. The contributions of other component parts of the aircraft, or of the various combinations of component parts for high-speed airplane configurations, however, are not well-understood. In order to provide such information, a series of investigations of models having various interchangeable component parts is being conducted in the Langley stability tunnel. The rotary derivatives are being determined by the rolling- and curved-flow techniques (see references 1 and 2) and the static-stability characteristics are being determined by conventional wind-tunnel procedures.

An investigation of the effects of vertical location of the horizontal tail relative to the wing on the low-speed static longitudinal stability and on the steady-state rotary damping in pitch for a swept-wing configuration is reported in reference 3. The present investigation, which is also for a swept-wing configuration, is concerned with the effects of horizontal tails of various sizes and at various tail lengths (when located on the fuselage center line) on the low-speed static longitudinal stability and on the steady-state rotary damping in pitch; some effects of fuselage fineness ratio and wing-fuselage interference also are considered. The rotary damping in pitch specifies the damping resulting only from curvature of the flight path, such as that obtained during a steady-pitching maneuver in which the radius of flight-path curvature is constant. For a pitching oscillation, the rotary damping derivative represents only a part of the total damping, since additional contributions may result from unsteady aerodynamic phenomena such as the lag of downwash between the wing and horizontal tail (references 4 and 5).

The model used in the present investigation had 45° sweptback wing and horizontal-tail surfaces with aspect ratios of 4. The model configurations tested for the present investigation represent certain specific combinations of the component parts of the general research model used in the investigations of static lateral stability derivatives reported in references 6 and 7.

SYMBOLS

The data presented herein are in the form of standard NACA coefficients of forces and moments which are referred to the stability system of axes, with the origin at the projection on the plane of symmetry of the quarter-chord point of the mean aerodynamic chord of the wing. The positive directions of the forces, moments, angles, and angular velocities are shown in figure 1. The coefficients and symbols are defined as follows:

C_L lift coefficient $\left(L/\frac{1}{2}\rho V^2 S_W\right)$

C_D drag coefficient $\left(D/\frac{1}{2}\rho V^2 S_W\right)$

C_m pitching-moment coefficient $\left(M/\frac{1}{2}\rho V^2 S_W \bar{c}_W\right)$

C_n yawing-moment coefficient $\left(N/\frac{1}{2}\rho V^2 S_W b_W\right)$

L lift, pounds

D drag, pounds

M pitching moment about $\bar{c}_W/4$, foot-pounds

N yawing moment about Z-axis, foot-pounds

ρ mass density, slugs per cubic foot

V velocity, feet per second

S area, square feet

b span, measured perpendicular to fuselage center line, feet

c chord, measured parallel to axis of symmetry, feet

$\bar{c}$ mean aerodynamic chord, feet $\left(\frac{2}{S}\int_0^{b/2} c^2\, dy\right)$

l tail length, distance from $\bar{c}_W/4$ to $\bar{c}_H/4$

A aspect ratio $\left(b^2/S\right)$

y spanwise distance from plane of symmetry, feet

λ taper ratio, ratio of tip chord to root chord

α angle of attack, measured in plane of symmetry, degrees

v_F fuselage volume

L_F fuselage length

d_F maximum fuselage diameter

ϵ effective downwash angle, degrees

ψ angle of yaw, degrees

q pitching angular velocity, radians per second

$\frac{qc}{2V}$ pitching-velocity parameter (based on $\bar{c}_W$)

$C_{L_\alpha} = \frac{\partial C_L}{\partial \alpha}$

$C_{m_\alpha} = \frac{\partial C_m}{\partial \alpha}$

$C_{m_q} = \frac{\partial C_m}{\partial \left(\frac{qc}{2V}\right)}$

$C_{n_\psi} = \frac{\partial C_n}{\partial \psi}$

$\left(\Delta C_{m_q}\right)_H$, $\left(\Delta C_{m_\alpha}\right)_H$ increment resulting from addition of horizontal tail (for example,

$$\left(\Delta C_{m_q}\right)_H = \left(C_{m_q}\right)_{\text{Model with H}} - \left(C_{m_q}\right)_{\text{Model without H}}$$

$\Delta_1 C_{m_q}$, $\Delta_1 C_{m_\alpha}$ increment resulting from interference effect of wing and fuselage (for example,

$$\Delta_1 C_{m_q} = \left(C_{m_q}\right)_{W+F} - \left(C_{m_q}\right)_W - \left(C_{m_q}\right)_F$$

Subscripts:

W	wing
F	fuselage
V	vertical tail
H	horizontal tail
r	radian measure

APPARATUS, MODELS, AND TESTS

The general research model used for the present investigation was designed to permit tests of the wing alone, fuselage alone, or the fuselage in combination with any of several tail configurations - with or without the wing. A sketch with some dimensions of the complete model with one particular tail configuration is shown in figure 2. A list of the pertinent geometric characteristics of various component parts is given in table I. All the parts were constructed of mahogany.

Three fuselages and three horizontal tails were used for the tests in various combinations with and without a wing. For convenience, each component is designated as follows:

W	Wing
F_1, F_2, F_3	Fuselages
V	Vertical tail
H_1, H_2, H_3	Horizontal tails

A complete list of the configurations investigated is presented in table II.

The three fuselages (fig. 3) were bodies of revolution having circular-arc profiles and fineness ratios of 5 for fuselage 1, 6.67 for fuselage 2, and 10 for fuselage 3. The wing and the three horizontal-tail surfaces all had aspect ratios of 4.0, taper ratios of 0.6, and NACA 65A008 airfoil sections parallel to the plane of symmetry; the quarter-chord lines were swept back 45°. Ordinates for the NACA 65A008 airfoil section are given in table III. The horizontal tails, the incidence of which was kept at 0° for all tests, differed from each other

only in area and are designated as H_1, H_2, and H_3 (in order of increasing size) in figure 4 and table I. The vertical tail had an aspect ratio of 1 and the quarter-chord line swept back 45°. Detailed dimensions of the vertical tail, however, are not considered pertinent to the present investigation.

A drawing of a complete model configuration is presented in figure 5 to illustrate the test setup in the tunnel. The model was rigidly mounted on a three-support-strut system with the pivot point 4 inches rearward of the quarter-chord point of the mean aerodynamic chord. Forces and moments were measured by means of a conventional six-component balance system.

The tests were made in the 6- by 6-foot test section of the Langley stability tunnel. The dynamic pressure for the tests was 24.9 pounds per square foot, which corresponds to a Mach number of 0.13 and to a Reynolds number based upon the wing mean aerodynamic chord of 0.71×10^6. The angle of attack was varied from about -6° to 30° for the tests. In addition to the straight-flow tests the tunnel flow was curved to obtain values of $qc/2V$ of 0.008, 0.017, and 0.022. The method of curving the flow consists in curving the tunnel walls to obtain the proper airstream curvature and inserting, upstream of the test section, screens which give the proper velocity gradient across the test section.

CORRECTIONS

The angle of attack and drag coefficient have been corrected for the effects of jet boundaries. The moment data have been transferred from the mounting point to the 25-percent point of the wing mean aerodynamic chord. The damping-in-pitch data have been corrected for the effects of the cross-tunnel static-pressure gradient associated with curved flow. The data have not been corrected for blocking, turbulence, or support-strut interference since, for the parameters with which this paper is concerned, these effects are believed to be negligible.

RESULTS AND DISCUSSION

Presentation of Results

The basic data obtained in the present investigation are presented in figures 6, 7, and 8. The effect of fuselage fineness ratio on the static longitudinal stability of the fuselage is summarized in figure 9; whereas the effect of tail size and tail length on the static longitudinal stability and damping in pitch contributed by the horizontal

tail is summarized in figure 10. The effect of wing-fuselage interference on both the static longitudinal stability and damping in pitch is shown in figure 11.

An index to the data for the configurations investigated is given in table II.

Static Longitudinal Stability

The static longitudinal stability characteristics for the wing and one complete model configuration are presented in figure 6. Inasmuch as these results are very similar to those presented in reference 6 and adequate analyses of the results are given in that reference, they are not discussed in this paper.

Data are not presented for the lift and drag of the model with each fuselage and horizontal tail investigated since the results showed that the lift and drag were only slightly affected by the changes in fuselage and tail. The lift and drag data presented in figure 6 for the configuration $W + F_2 + V + H_2$ are representative of the lift and drag results for all the complete model configurations.

The pitching-moment characteristics of the three isolated fuselages are presented as a function of angle of attack in figure 7 and are summarized for $\alpha = 0^\circ$ in figure 9. In order that the results obtained may be applied conveniently to arbitrary airplane configurations, coefficients in terms of fuselage dimensions rather than wing dimensions are needed. This manner of expressing the coefficient is accomplished by plotting the quantity $\left(C_{m_\alpha}\right)_F \frac{S_W \bar{c}_W}{v_F}$ against fuselage fineness ratio $\frac{L_F}{d_F}$. The quantity plotted, therefore, is effectively the pitching-moment coefficient based upon fuselage volume v_F. For a body of revolution at a angle of attack of 0°, the value $\left(C_{m_\alpha}\right)_F \frac{S_W \bar{c}_W}{v_F}$ is the same as $\left(C_{n_\psi}\right)_F \frac{S_W b_W}{v_F}$; therefore, the results from the present investigation can be compared with the directional stability data presented in figure 16 of reference 7. The data from the present tests show the same trend as the data of reference 7 but are somewhat larger in magnitude. The difference probably results from the different methods for supporting the models in the tunnel. Comparison of the test data with calculations made by the classical theory of reference 8 shows that, although the

variation with fineness ratio is generally similar, the magnitude of the test values is only about four-fifths of that predicted by theory.

Addition of any of the fuselages to the wing had little effect on C_{m_α}, as can be seen by comparison of figures 6 and 8. The fact that the wing-fuselage combination had approximately the same longitudinal stability as the wing alone may be attributed to the loss in load over the wing near the wing-fuselage juncture and to the alteration in fuselage loading effected by upwash in front of the wing.

The contribution of the horizontal tail to the static longitudinal stability can be expressed by the following conventional relation, if variations in dynamic pressure and fuselage interference are neglected and provided that the downwash parameter $\frac{\partial \epsilon}{\partial \alpha}$ can be evaluated:

$$\left(\Delta C_{m_\alpha}\right)_H = \left(C_{L_\alpha}\right)_H \left(1 - \frac{\partial \epsilon}{\partial \alpha}\right) \frac{S_H}{S_W} \frac{l}{\bar{c}_W} \tag{1}$$

As can be seen from equation (1), the tail contribution to static longitudinal stability is proportional to the geometric quantity $\frac{S_H}{S_W} \frac{l}{\bar{c}_W}$, the experimental data have accordingly been plotted against this quantity in figure 10(a) for an angle of attack equal to 0°. The dashed curves in figure 10(a) were calculated by means of equation (1) by assuming various arbitrary values of the downwash parameter $\frac{\partial \epsilon}{\partial \alpha}$. In the calculations, the tail lift-curve slope $\left(C_{L_\alpha}\right)_H$ was assumed to have the value of 0.054 obtained for the wing alone (fig. 6) since the wing and tail have the same plan form and section. From the data in figure 10(a), it can be seen that, for the wing-off configurations, the experimental points nearly fall on the $\frac{\partial \epsilon}{\partial \alpha} = 0$ curve. The slight difference between these points and the curve indicates that the fuselage probably had some influence on the tail effectiveness. With the wing on, however, the data indicate that $\frac{\partial \epsilon}{\partial \alpha}$ for the range of model configurations considered in this investigation is about 0.52. This value is only slightly affected by changes in tail length and size. The data in figure 10(a) also show that, as indicated by equation (1), the contribution of the horizontal tail to static longitudinal stability varies linearly with tail area and tail length.

For configurations including the wing, a destabilizing change in the slope C_{m_α} generally occurs at an angle of attack of about 10°. For the shortest tail length (fuselage F_1, fig. 8(a)) the magnitude of

this change in slope apparently was increased slightly as the horizontal-tail area was increased. For the longest tail length (fuselage F_3, fig. 8(c)) an increase in tail area caused a decrease in this destabilizing change in slope; in fact, this change apparently was eliminated by the addition of the two largest tails (H_2 or H_3). This effect of tail length on the manner in which addition of tail area affects the longitudinal stability appears to be primarily a matter of geometry, in that, for a given location of the tail relative to the fuselage center line, the tail length determines the vertical location of the tail relative to the wing wake at a particular angle of attack. The destabilizing tendency for the wing-fuselage combination at an angle of attack of about 10° results from tip stalling, and, as a result of this stalling, the wing trailing vortices move inward with an associated increase in downwash in the wake at the plane of symmetry. For the short tail length the tail is sufficiently close to the wake at an angle of attack of 10° to experience destabilizing effect. For the longest tail length, however, the tail has emerged sufficiently from the wake to avoid the effect of the increased downwash.

The data in figure 8 show that the static longitudinal stability was generally greater at angles of attack near the stall than for any other part of the angle-of-attack range.

Damping in Pitch

The steady-state rotary damping in pitch for the wing alone is presented in figure 6. The values of C_{m_q} are generally in good agreement with theoretical values determined by methods presented in reference 9 and the variation with angle of attack is of little significance. Addition of a fuselage to the wing did not affect the value of C_{m_q} appreciably for angles of attack up to the stall (compare figs. 6 and 8). This effect was similar to that found for the static longitudinal stability of the model.

The damping-in-pitch results presented in figure 7 for the isolated fuselages are considered to be of qualitative value only, since the accuracy of the measurements is not considered sufficient to yield results of a reasonable percentage accuracy for damping values as low as those given by the fuselages. The indications are, however, that the fuselages produced damping of the same sign as that normally expected for a horizontal tail and that the variation of the fuselage damping with angle of attack was not particularly significant.

At low angles of attack, the increment in the rotary damping in pitch due to horizontal tail can be expressed by the formula developed in reference 3 as follows, if variations in dynamic pressure and fuselage interference are neglected and provided that the downwash-due-to-pitching parameter $\frac{\partial \epsilon_r}{\partial \frac{ql}{V}}$ can be evaluated:

$$\left(\Delta C_{m_q}\right)_H = -114.6\left(C_{L_\alpha}\right)_H\left(1 - \frac{\partial \epsilon_r}{\partial \frac{ql}{V}}\right)\frac{S_H}{S_W}\left(\frac{l}{\bar{c}_W}\right)^2 \qquad (2)$$

where ϵ_r is downwash angle in radian measure. As indicated by equation (2), the tail contribution to the damping in pitch is proportional to $\frac{S_H}{S_W}\left(\frac{l}{\bar{c}_W}\right)^2$, and the experimental data have, accordingly, been plotted against this quantity in figure 10(b) for an angle of attack equal to 0°. The dashed curves were calculated by means of equation (2) by assuming arbitrary values of $\frac{\partial \epsilon_r}{\partial \frac{ql}{V}}$. The value of $\left(C_{L_\alpha}\right)_H$ was assumed equal to 0.054 as discussed in the preceding section.

The fact that the experimental points obtained with the wing removed do not coincide exactly with the curve for $\frac{\partial \epsilon_r}{\partial \frac{ql}{V}} = 0$ indicates that the fuselage probably had some influence on the tail effectiveness. The data in figure 10(b), however, indicate that, in general, the downwash had practically no effect on the steady-state damping in pitch so that $\frac{\partial \epsilon_r}{\partial \frac{ql}{V}}$ can be assumed to be zero. The positions of the test values for the wing-on conditions relative to those for the wing-off conditions indicate, in fact, that the wing contributed a slightly negative value of $\frac{\partial \epsilon_r}{\partial \frac{ql}{V}}$; thus, an increase in the tail effectiveness for damping in pitch resulted. A slight increase in tail effectiveness due to the presence of the wing might be expected as a result of the unusual downwash pattern behind a sweptback wing in pitching flight as is explained in reference 3.

The data in figure 10(b) also show that, as indicated in equation (2), the contribution of the horizontal tail to the rotary damping in pitch varies linearly with tail area and with the square of tail length.

For the wing-off configurations, as the angle of attack increases, the damping in pitch contributed by the horizontal tail generally decreases (fig. 7). With the wing on, however, the damping in pitch reaches a maximum value at some moderate angle of attack, then decreases with further increase in angle of attack such that, near the stall (approximately 24°), the damping in pitch is less than at an angle of attack of 0°. It is interesting to note that the angle of attack at which maximum damping occurs generally decreases with increasing fuselage length; this trend can best be seen by comparing the curves for the large tail on the various fuselages (fig. 8). Since most of the damping is due to the horizontal tail, any changes in the damping with angle of attack which are caused by the tail are likely to become greater with increasing tail size.

Wing-Fuselage Interference

The data obtained in the investigation of the horizontal-tail effect also make possible an evaluation of the interference increments ($\Delta_1 C_{m_\alpha}$ and $\Delta_1 C_{m_q}$) which enter into the following equations for total values of the static-longitudinal-stability and damping-in-pitch derivatives for complete airplane configurations:

$$\left(C_{m_\alpha}\right)_{Total} = \left(C_{m_\alpha}\right)_W + \left(C_{m_\alpha}\right)_F + \Delta_1 C_{m_\alpha} + \left(\Delta C_{m_\alpha}\right)_H$$

$$\left(C_{m_q}\right)_{Total} = \left(C_{m_q}\right)_W + \left(C_{m_q}\right)_F + \Delta_1 C_{m_q} + \left(\Delta C_{m_q}\right)_H$$

where $\left(\Delta C_{m_\alpha}\right)_H$ and $\left(\Delta C_{m_q}\right)_H$ are the values for the horizontal tail in the presence of the wing and fuselage. The values $\Delta_1 C_{m_\alpha}$ and $\Delta_1 C_{m_q}$ result from interference between the wing and fuselage (that is, $\Delta_1 C_{m_q} = \left(C_{m_q}\right)_{W+F} - \left(C_{m_q}\right)_W - \left(C_{m_q}\right)_F$). The interference increments usually are assumed to apply to airplanes having configurations somewhat similar to that of the model used in evaluating the increments. The height of the wing relative to the fuselage center line usually has a significant effect on the magnitude of the interference increments. Since, for the present investigation, the wing was located on the fuselage center line, the results are considered applicable only to midwing or near midwing arrangements.

The increments are presented in figure 11 as functions of angle of attack. Within the accuracy of the determinations there appeared to be no consistent effect of fuselage length on either $\Delta_1 C_{m_\alpha}$ or $\Delta_1 C_{m_q}$ and, for the purposes for which these values were intended to be used, the use of a faired value to represent the effect of interference seems reasonable. The variation of $\Delta_1 C_{m_\alpha}$ with angle of attack is small below 16° and the average value tends to increase the stability. The variation of $\Delta_1 C_{m_q}$ with angle of attack is not appreciable over the entire angle-of-attack range and the average value tends to decrease the damping.

CONCLUSIONS

The results of an investigation to determine the effect of horizontal-tail size and tail length, when the tail is located at the center line of the fuselage, on the static longitudinal stability and the steady-state rotary damping in pitch of a complete model with wing and tail surfaces having the quarter-chord lines swept back 45° and an aspect ratio of 4 indicate the following conclusions:

1. The contribution of the horizontal tail to static longitudinal stability and damping in pitch was in agreement with analytic considerations in that the contribution of the horizontal tail to static longitudinal stability was related directly to the tail size and length; whereas its contribution to damping in pitch was related directly to tail size and the square of tail length.

2. At low angles of attack, the contribution of the horizontal tail to static longitudinal stability was decreased by about one-half by addition of the wing; whereas the contribution of the horizontal tail to the rotary damping in pitch was almost unaffected by the addition of the wing, regardless of the tail area or tail length.

3. The static longitudinal stability near the stall was slightly greater than at an angle of attack of 0°; whereas the damping in pitch was somewhat less near the stall than at an angle of attack of 0°.

4. At an angle of attack of about 10°, the static longitudinal stability of the wing-fuselage combinations changed adversely. The magnitude of this change was slightly increased by the addition of tail area at the shortest tail length but was decreased by the addition of tail area at the longest tail length.

Langley Aeronautical Laboratory
National Advisory Committee for Aeronautics
Langley Field, Va., March 27, 1951.

REFERENCES

1. MacLachlan, Robert, and Letko, William: Correlation of Two Experimental Methods of Determining the Rolling Characteristics of Unswept Wings. NACA TN 1309, 1947.

2. Goodman, Alex, and Brewer, Jack D.: Investigation at Low Speeds of the Effect of Aspect Ratio and Sweep on Static and Yawing Stability Derivatives of Untapered Wings. NACA TN 1669, 1948.

3. Lichtenstein, Jacob H.: Effect of Horizontal-Tail Location on Low-Speed Static Longitudinal Stability and Damping in Pitch of a Model Having 45° Sweptback Wing and Tail Surfaces. NACA TN 2381, 1951.

4. Cowley, W. L., and Glauert, H.: The Effect of the Lag of the Downwash on the Longitudinal Stability of an Aeroplane and on the Rotary Derivative M_q. R. & M. No. 718, British A.R.C., 1921.

5. Jones, Robert T., and Fehlner, Leo F.: Transient Effects of the Wing Wake on the Horizontal Tail. NACA TN 771, 1940.

6. Brewer, Jack D., and Lichtenstein, Jacob H.: Effect of Horizontal Tail on Low-Speed Static Lateral Stability Characteristics of a Model Having 45° Sweptback Wing and Tail Surfaces. NACA TN 2010, 1950.

7. Queijo, M. J., and Wolhart, Walter D.: Experimental Investigation of the Effect of Vertical-Tail Size and Length and of Fuselage Shape and Length on the Static Lateral Stability Characteristics of a Model with 45° Sweptback Wing and Tail Surfaces. NACA TN 2168, 1950.

8. Munk, Max M.: The Aerodynamic Forces on Airship Hulls. NACA Rep. 184, 1924.

9. Toll, Thomas A., and Queijo, M. J.: Approximate Relations and Charts for Low-Speed Stability Derivatives of Swept Wings. NACA TN 1581, 1948.

TABLE I

PERTINENT GEOMETRIC CHARACTERISTICS OF THE MODEL

Fuselage:	F_1	F_2	F_3
Length, inches	30	40	60
Fineness ratio	5	6.67	10
Tail length, inches	12.53	16.70	25.05
Tail-length ratio, $l/\bar{c}_W$	1.36	1.82	2.73
Volume, v_F, cubic feet	0.267	0.350	0.526

Wing:	
Aspect ratio, A_W	4.0
Taper ratio, λ_W	0.6
Quarter-chord sweep angle, degrees	45
Dihedral angle, degrees	0
Twist, degrees	0
NACA airfoil section	65A008
Area, S_W, square inches	324
Span, b_W, inches	36
Mean aerodynamic chord, $\bar{c}_W$, inches	9.19

Horizontal tail:	H_1	H_2	H_3
Aspect ratio, A_H	4.0	4.0	4.0
Taper ratio, λ_H	0.6	0.6	0.6
Quarter-chord sweep angle, degrees	45	45	45
Dihedral angle, degrees	0	0	0
Twist, degrees	0	0	0
NACA airfoil section	65A008	65A008	65A008
Area, S_H, square inches	32.40	64.80	97.20
Span, b_H, inches	11.38	16.10	19.72
Mean aerodynamic chord, $\bar{c}_H$, inches	2.91	4.11	5.04
Area ratio, S_H/S_W	0.10	0.20	0.30

TABLE II

CONFIGURATIONS INVESTIGATED AND INDEX TO THE FIGURES HAVING DATA FOR THE CONFIGURATIONS

Wing off		Wing on	
Configuration[1]	Figure	Configuration[1]	Figure
----------	--------	W	6
F_1	7(a)	W + F_1	8(a)
----------	--------	W + F_1 + V + H_1	8(a), 10
F_1 + V + H_2	7(a), 10	W + F_1 + V + H_2	8(a), 10
----------	--------	W + F_1 + V + H_3	8(a), 10
F_2	7(b)	W + F_2	8(b)
----------	--------	W + F_2 + V + H_1	8(b), 10
F_2 + V + H_2	7(b), 10	W + F_2 + V + H_2	6, 8(b), 10
----------	--------	W + F_2 + V + H_3	8(b), 10
F_3	7(c)	W + F_3	8(c)
----------	--------	W + F_3 + V + H_1	8(c), 10
F_3 + V + H_2	7(c), 10	W + F_3 + V + H_2	8(c), 10
----------	--------	W + F_3 + V + H_3	8(c), 10

[1]Notation:

W wing
F fuselage
V vertical tail
H horizontal tail

For details see figures 2 to 4. Subscripts 1, 2, and 3 refer to size.

TABLE III

ORDINATES FOR NACA 65A008 AIRFOIL

[Stations and ordinates in percent airfoil chord]

Station	Ordinate
0	0
.50	.62
.75	.75
1.25	.95
2.50	1.30
5.00	1.75
7.50	2.12
10	2.43
15	2.93
20	3.30
25	3.59
30	3.79
35	3.93
40	4.00
45	3.99
50	3.90
55	3.71
60	3.46
65	3.14
70	2.76
75	2.35
80	1.90
85	1.43
90	.96
95	.49
100	.02
L.E. radius:	0.408

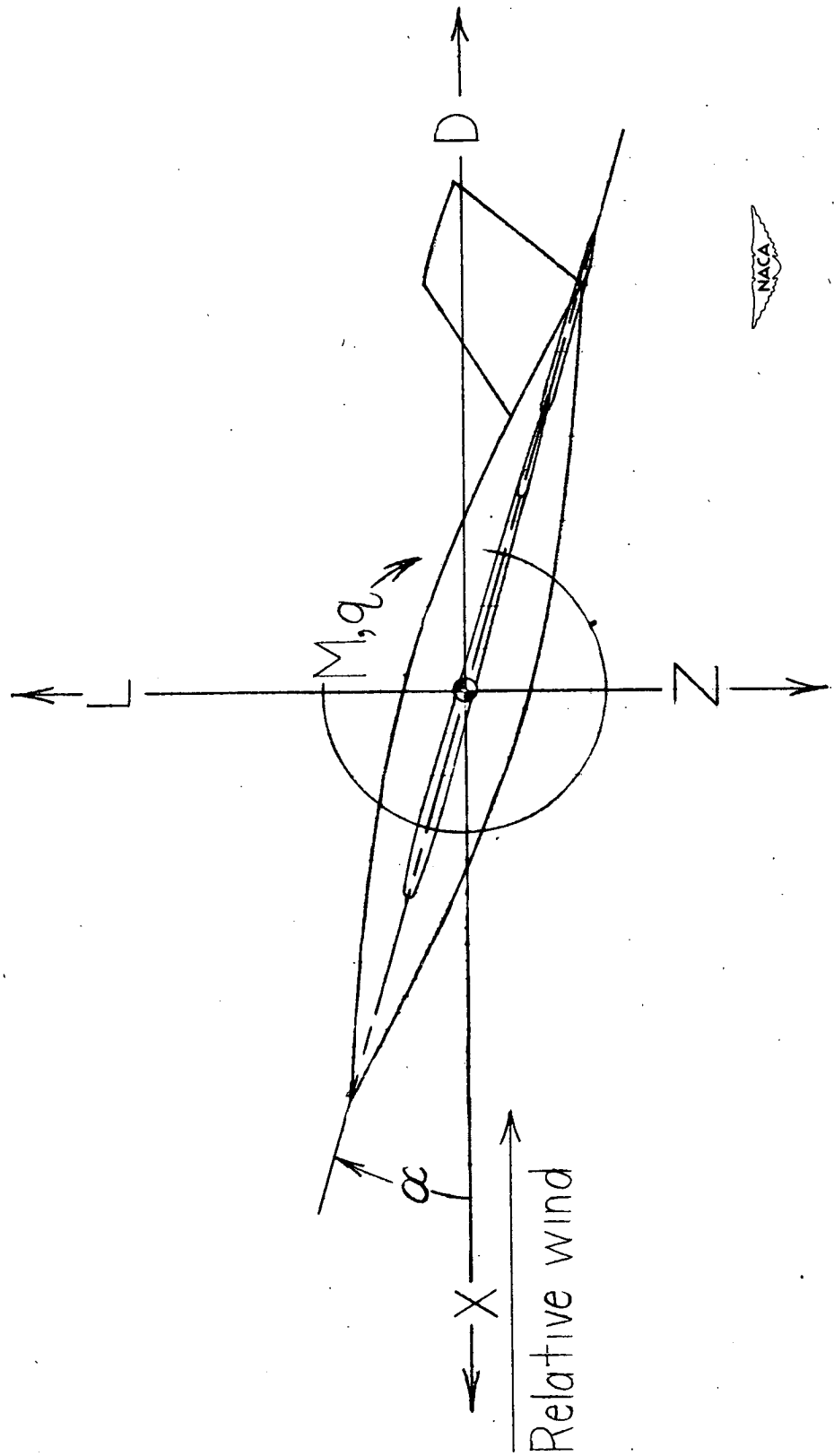

Figure 1.- System of axes used. Arrows indicate positive direction of forces, moments, angles, and angular velocities.

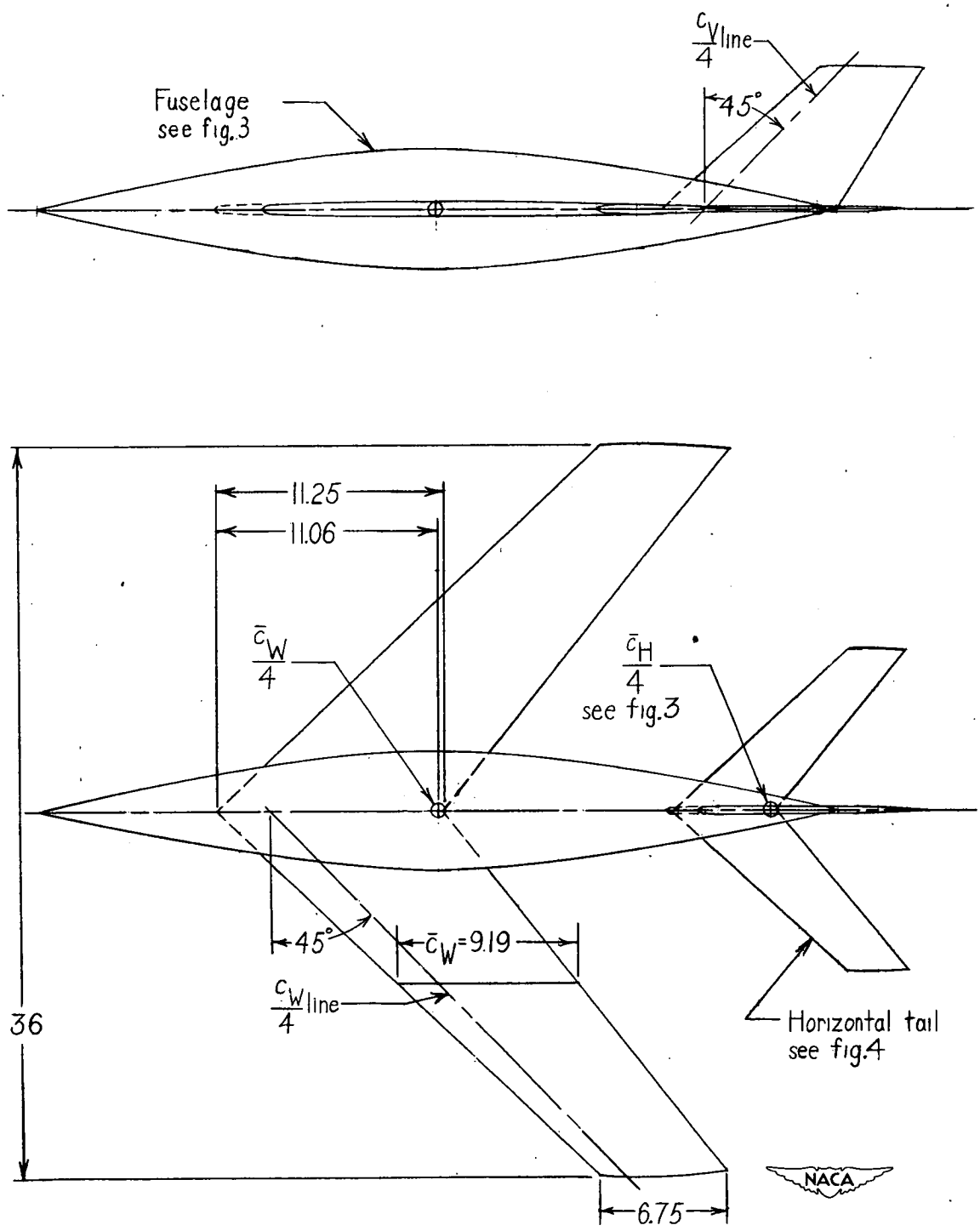

Figure 2.- Dimensions of the complete model. All dimensions are in inches.

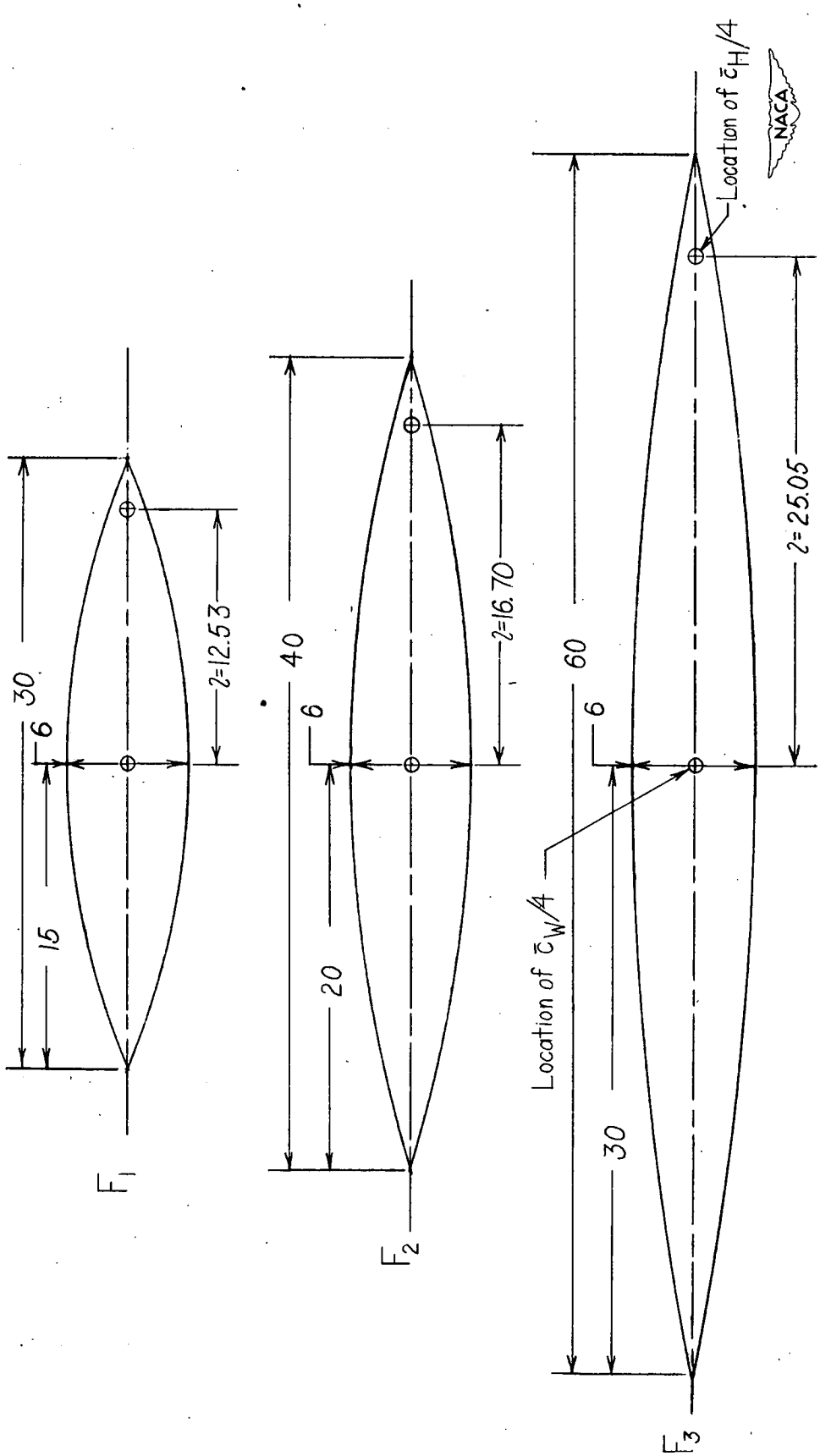

Figure 3.- Dimensions of the fuselages tested. All dimensions are in inches.

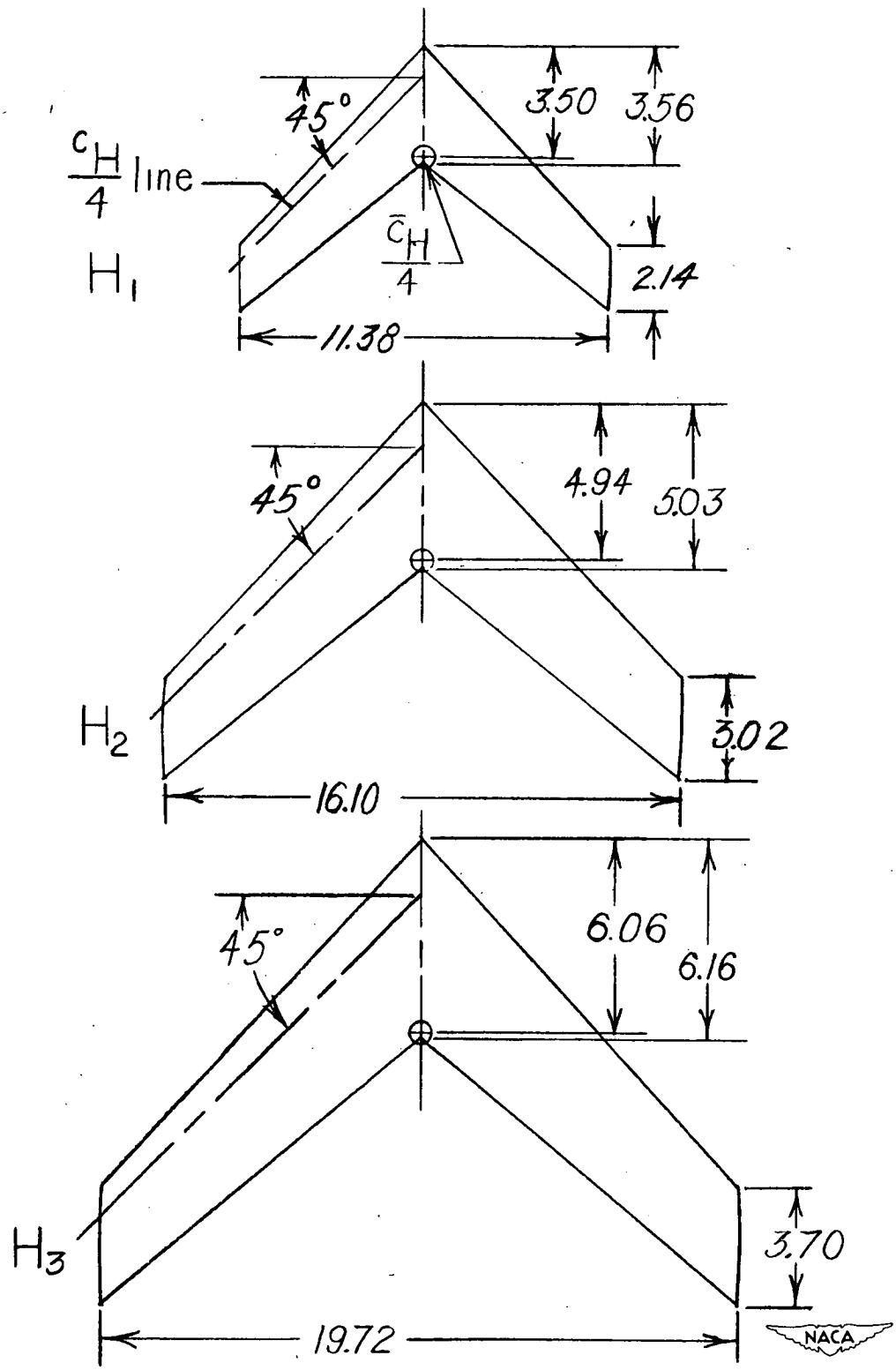

Figure 4.- Dimensions of the horizontal tails tested. All dimensions are in inches.

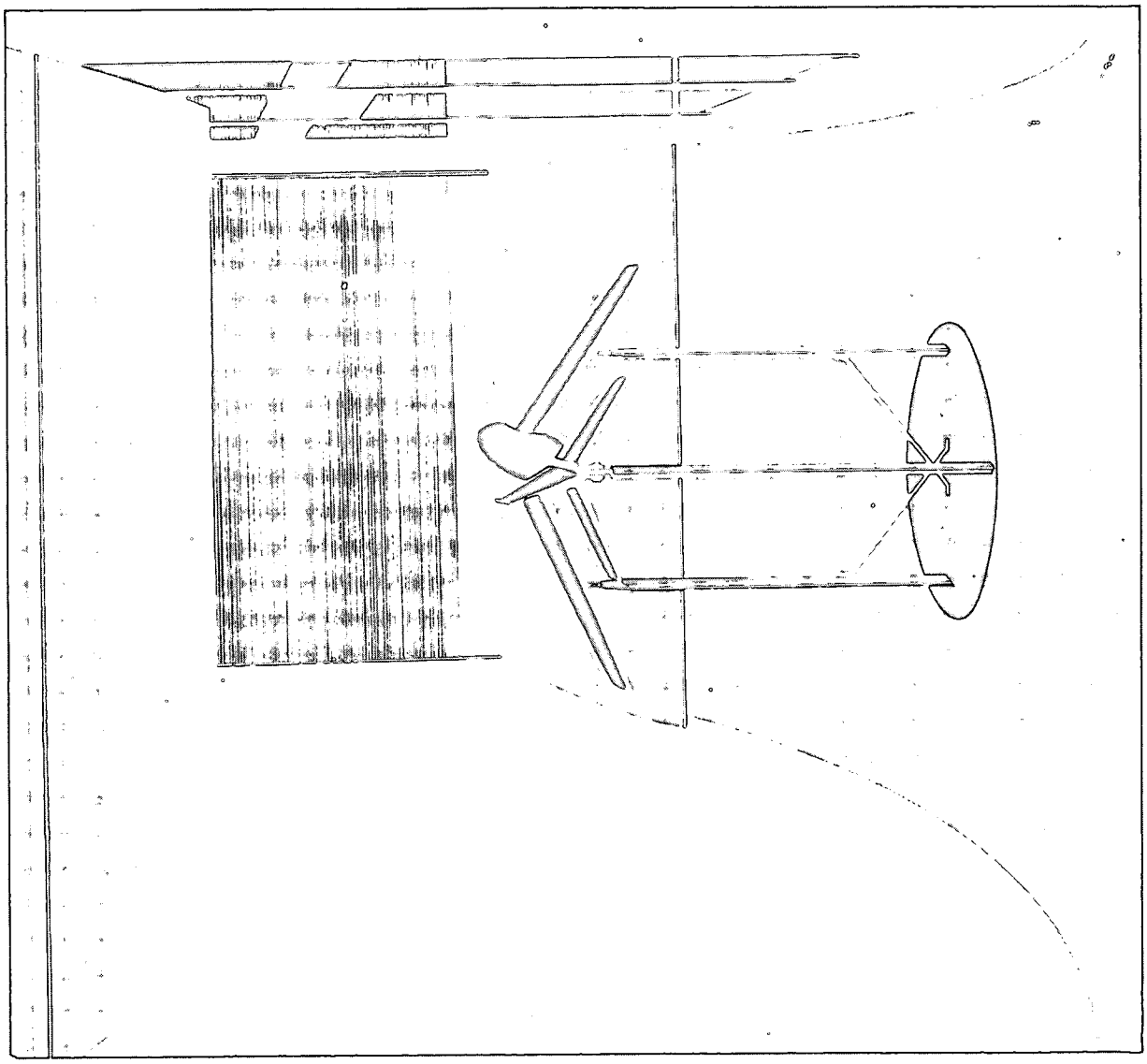

L-69122

Figure 5.- Drawing of a complete model configuration as mounted in the Langley stability tunnel for testing in curved flow.

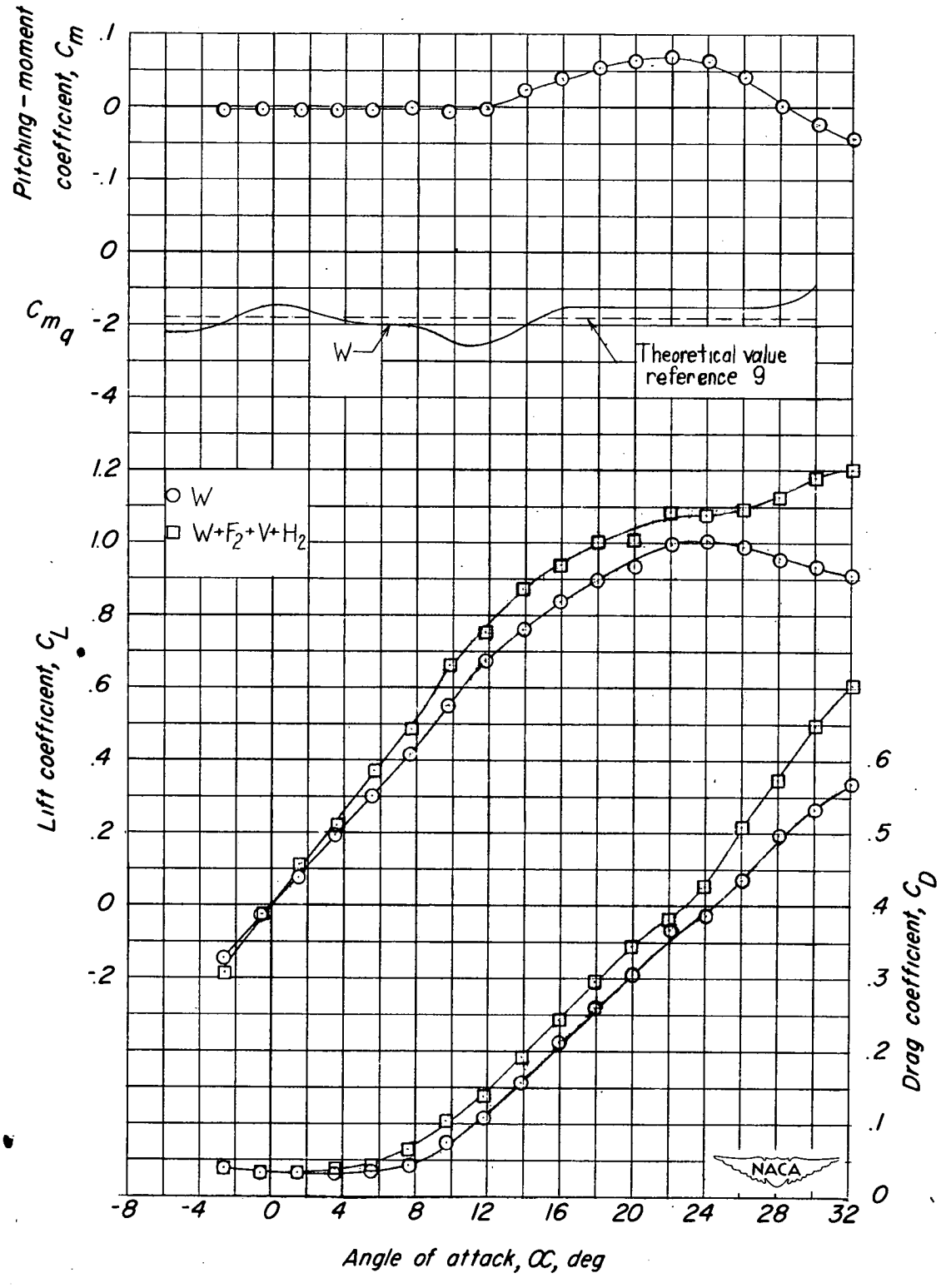

Figure 6.- Aerodynamic characteristics of the wing alone and of a typical complete model configuration.

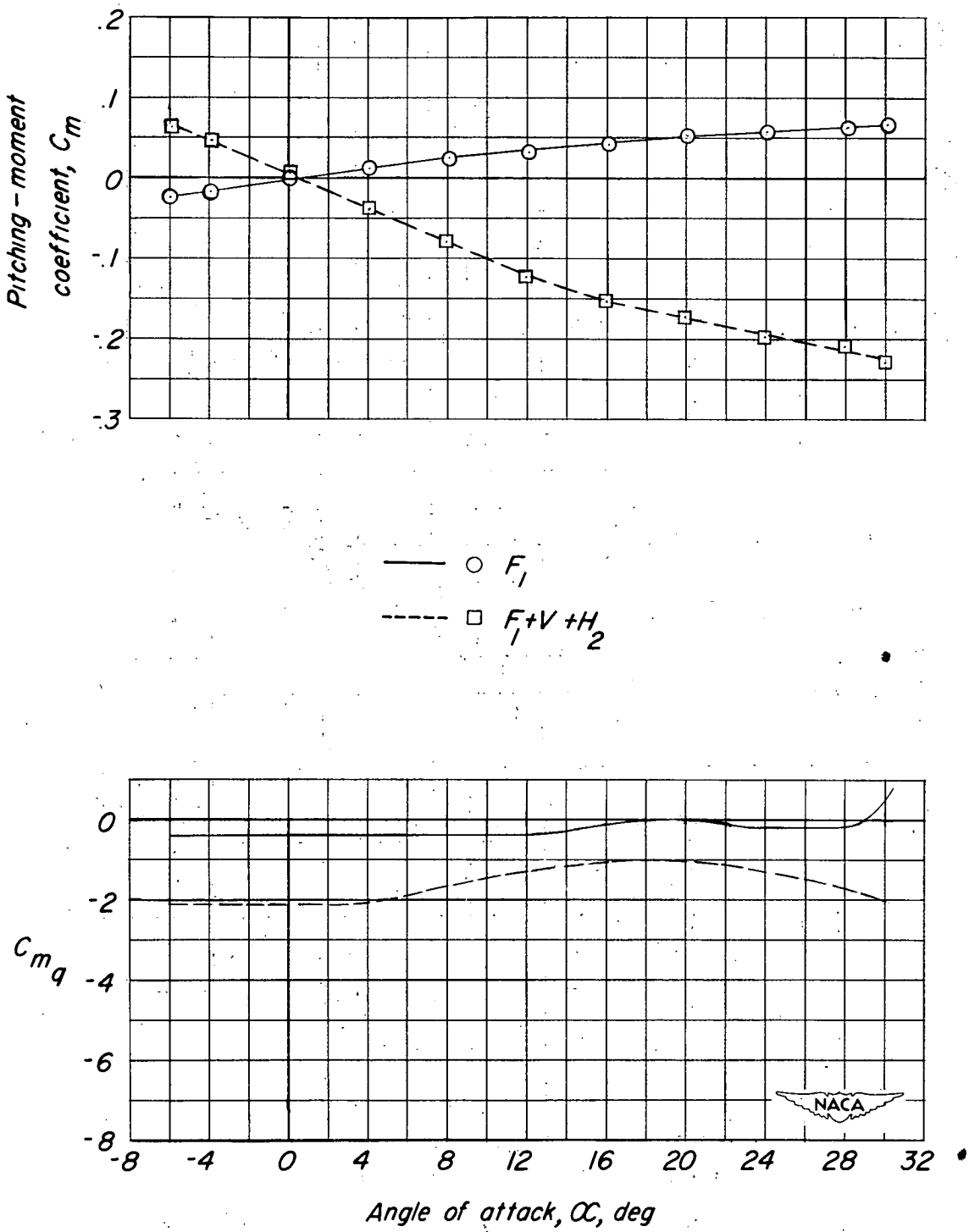

(a) Short fuselage F_1.

Figure 7.- Variation of C_m and C_{m_q} with angle of attack for the wing-off configurations.

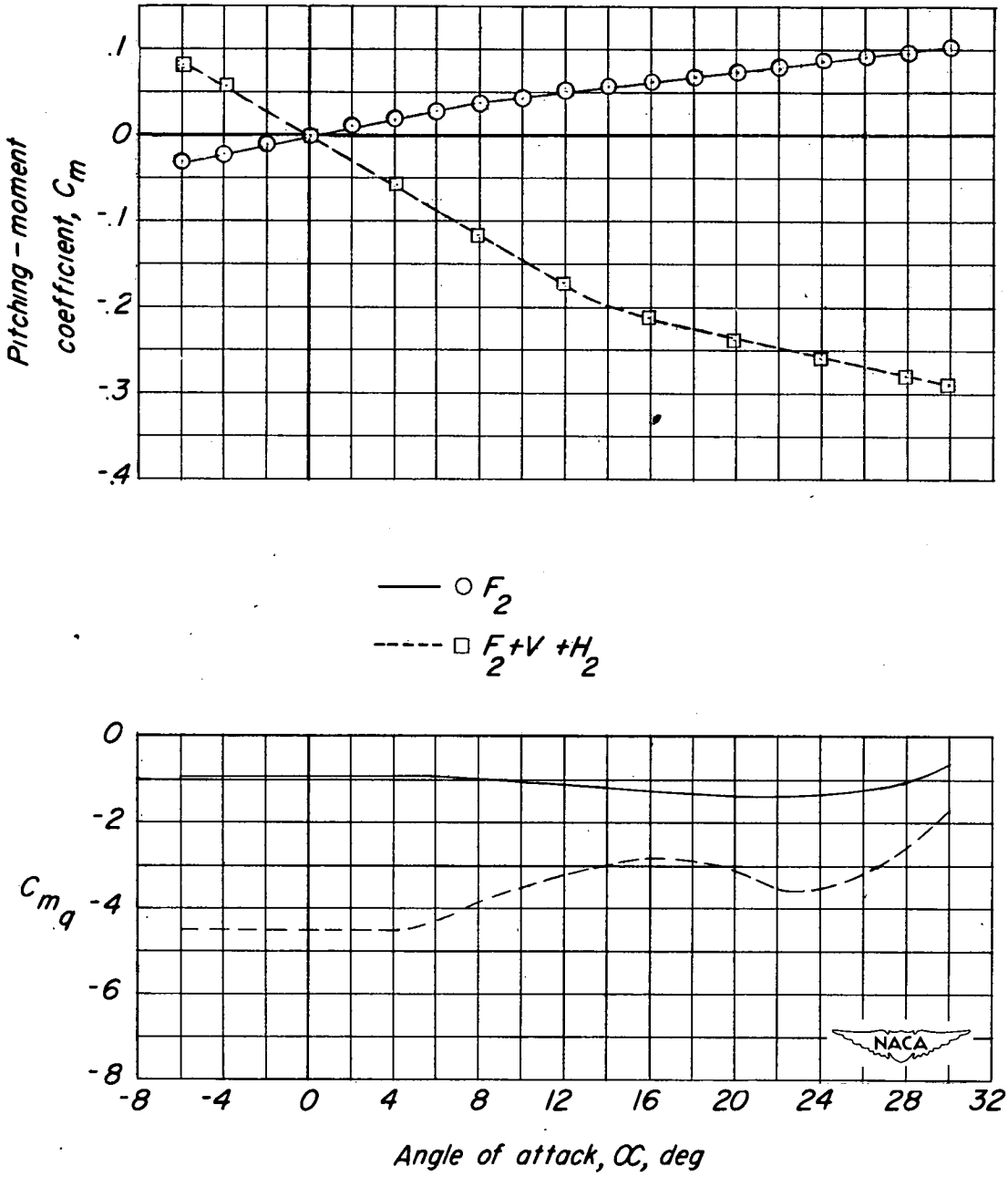

(b) Medium fuselage F_2.

Figure 7.- Continued.

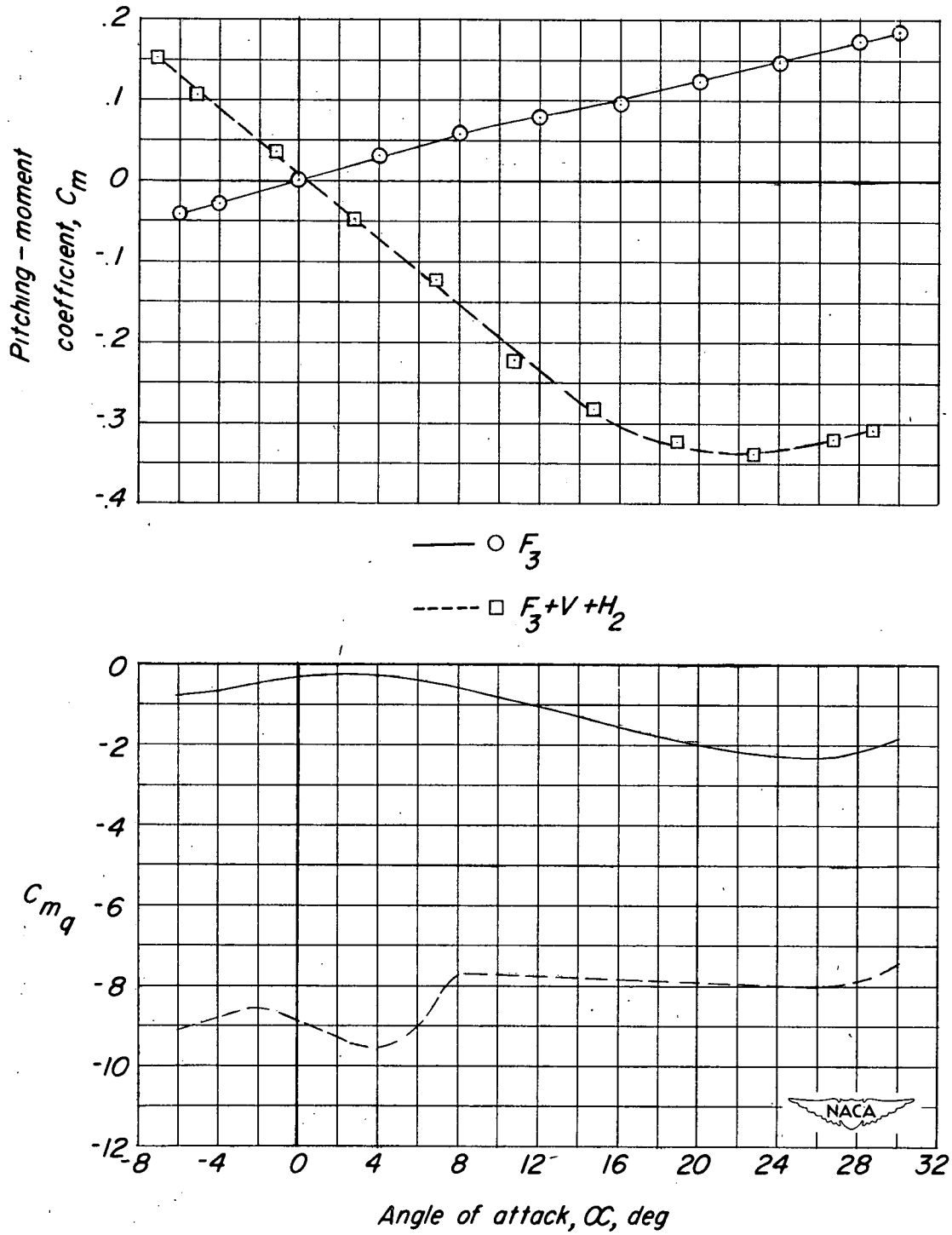

(c) Long fuselage F_3.

Figure 7.- Concluded.

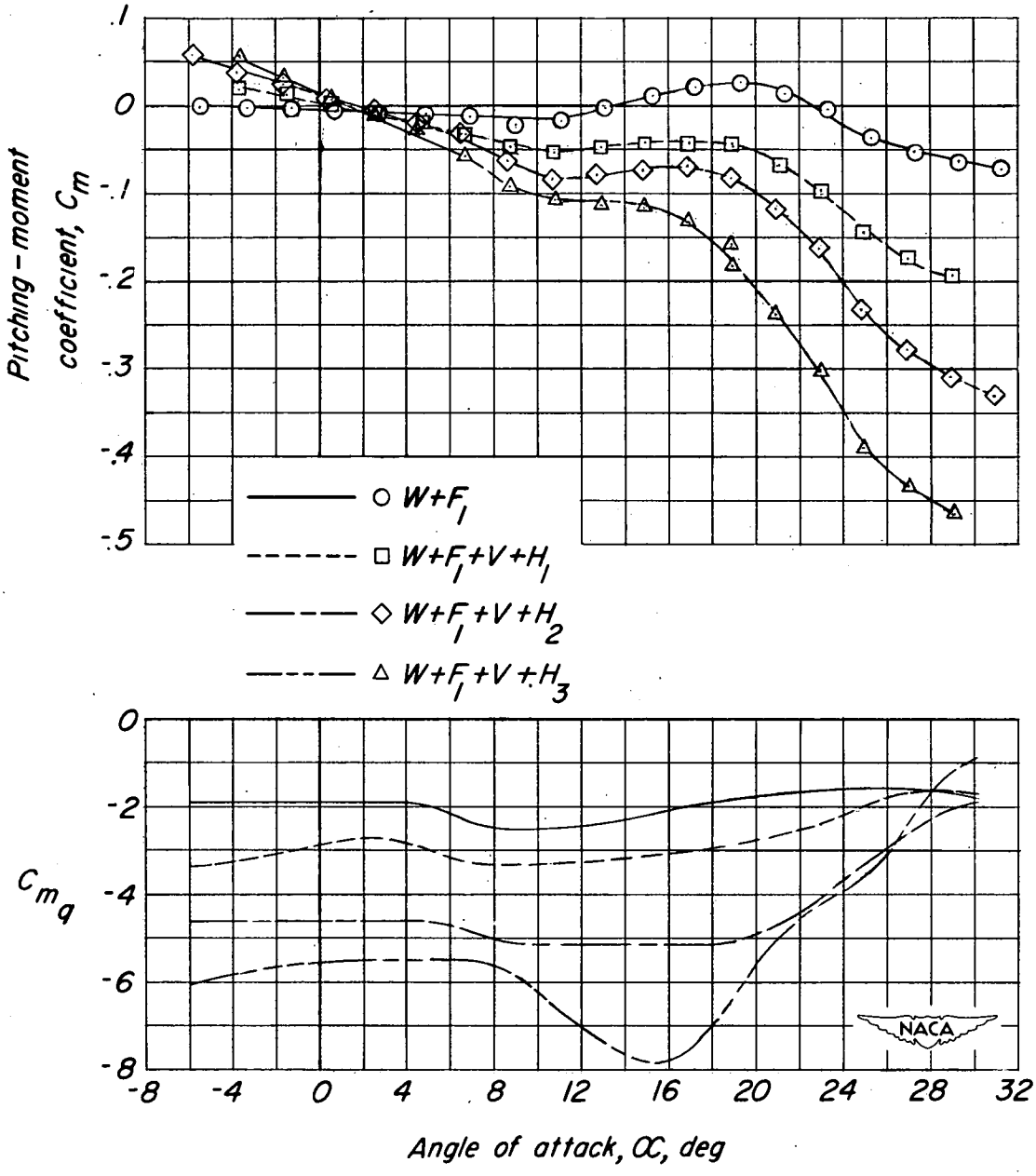

(a) Short fuselage F_1.

Figure 8.- Variation of C_m and C_{m_q} with angle of attack for the various complete model configurations.

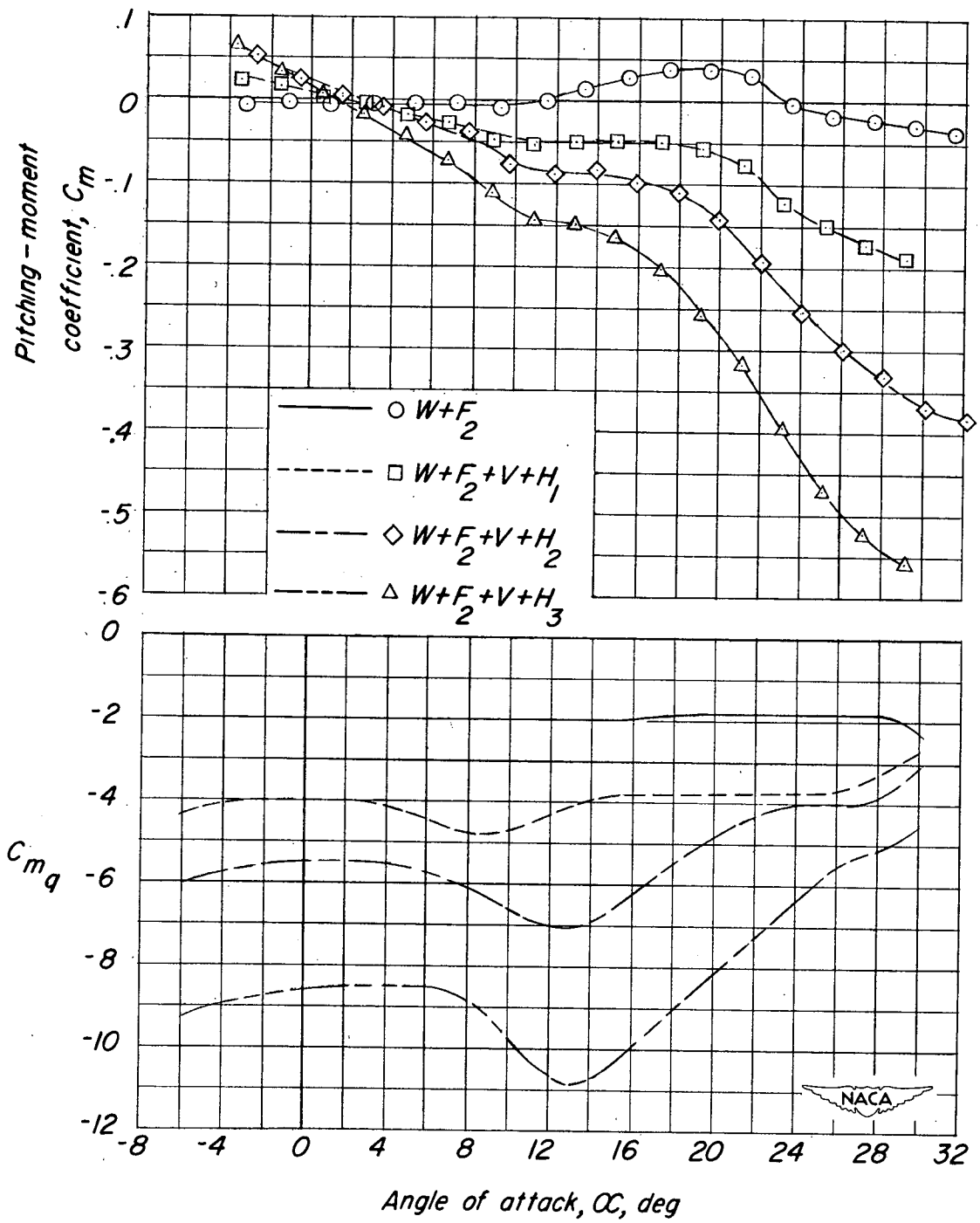

(b) Medium fuselage F_2.

Figure 8.- Continued.

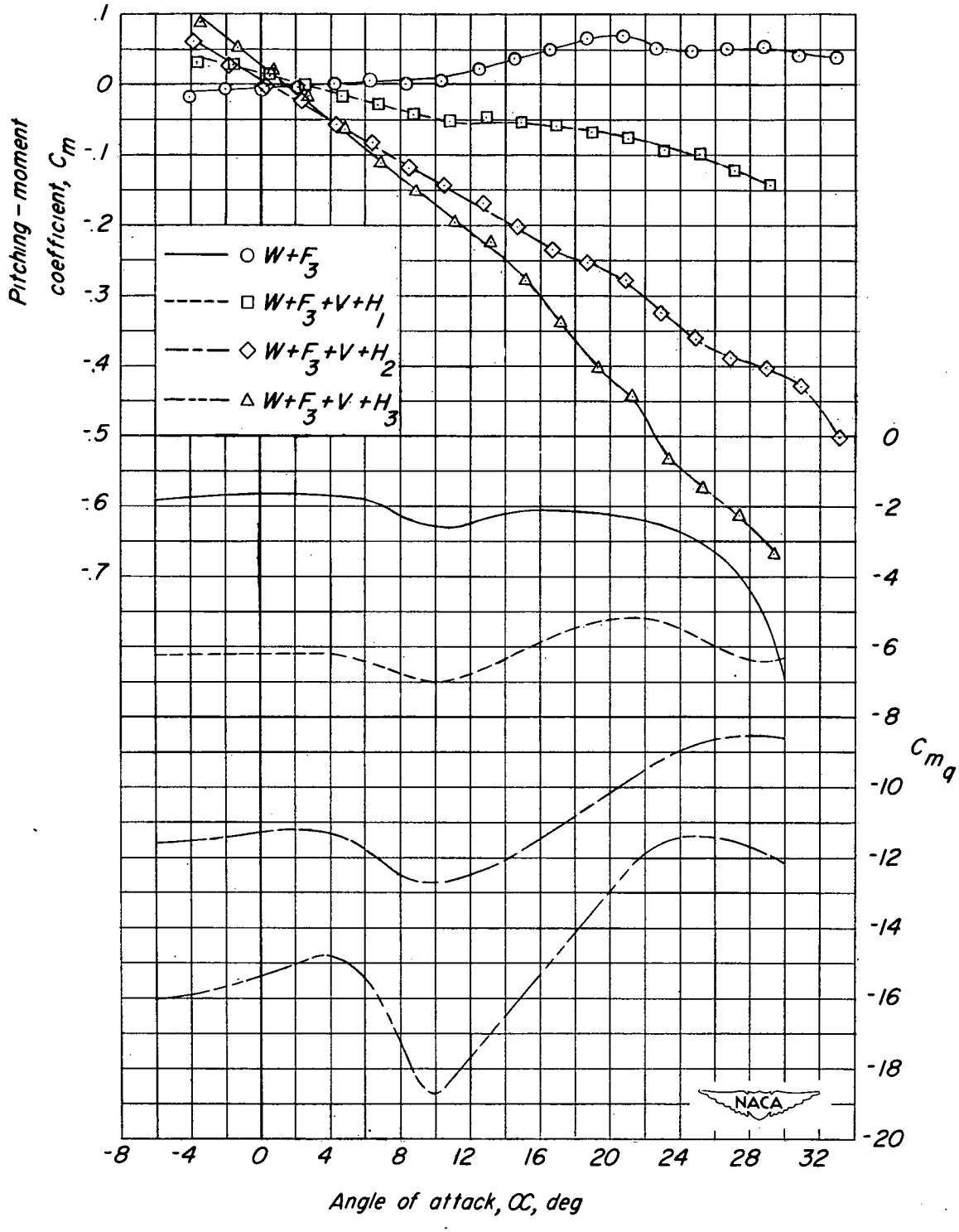

(c) Long fuselage F_3.

Figure 8.- Concluded.

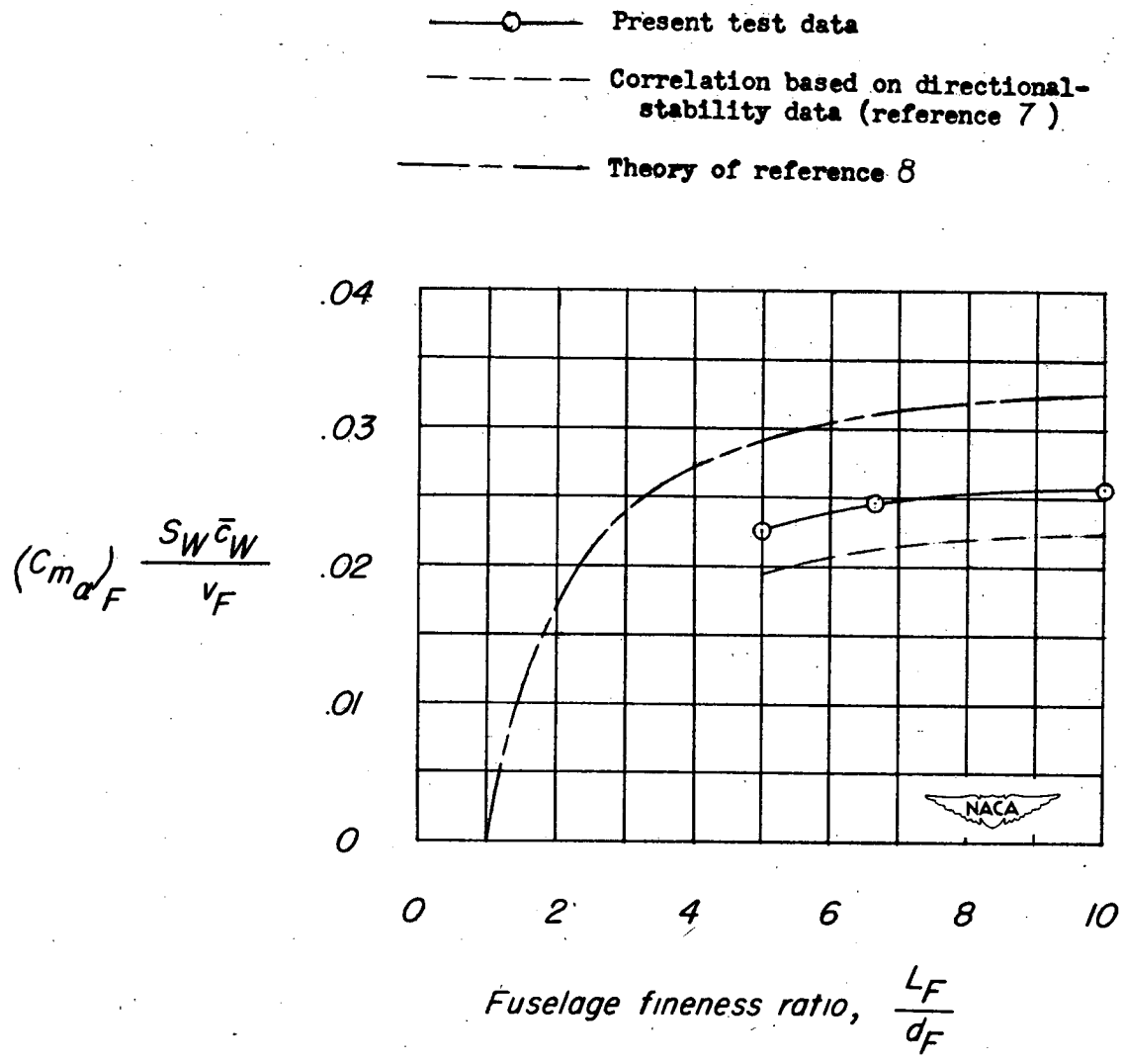

Figure 9.- Comparison of the effect of fuselage fineness ratio on the static stability of the fuselage as determined from longitudinal- and directional-stability measurements and from theory. $\alpha = 0^\circ$.

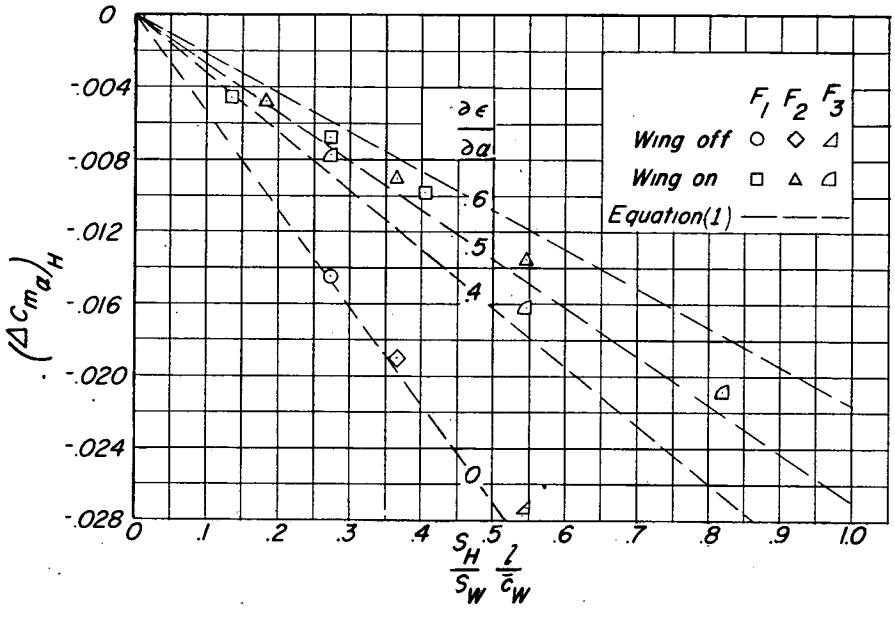

(a) Variation of $\left(\Delta C_{m_\alpha}\right)_H$ with $\frac{S_H}{S_W}\frac{l}{\bar{c}_W}$.

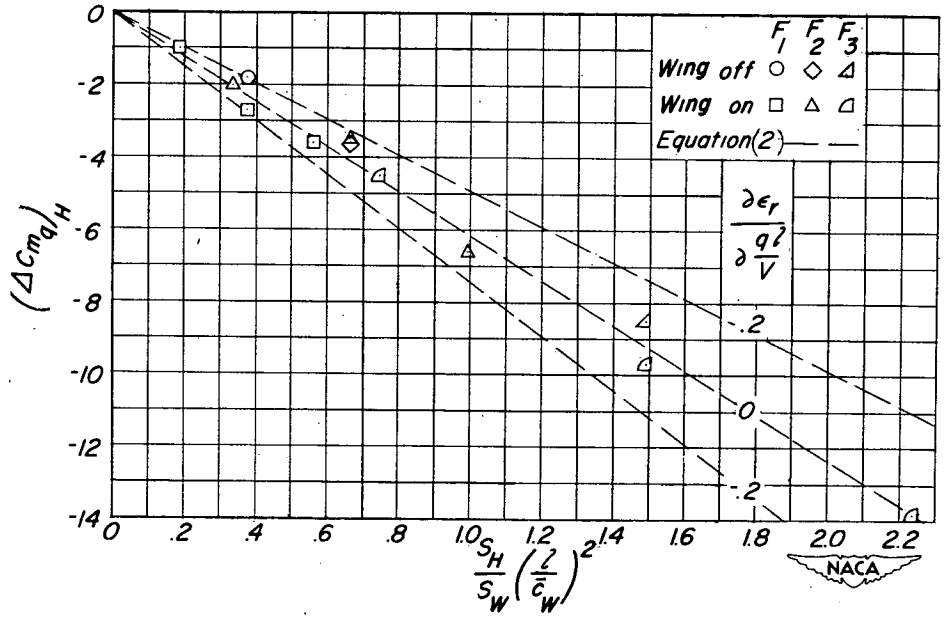

(b) Variation of $\left(\Delta C_{m_q}\right)_H$ with $\frac{S_H}{S_W}\left(\frac{l}{\bar{c}_W}\right)^2$.

Figure 10.- Summary of horizontal-tail contributions to static longitudinal stability and to damping in pitch. $\alpha = 0^\circ$. Like symbols indicate different horizontal tails on the same fuselage.

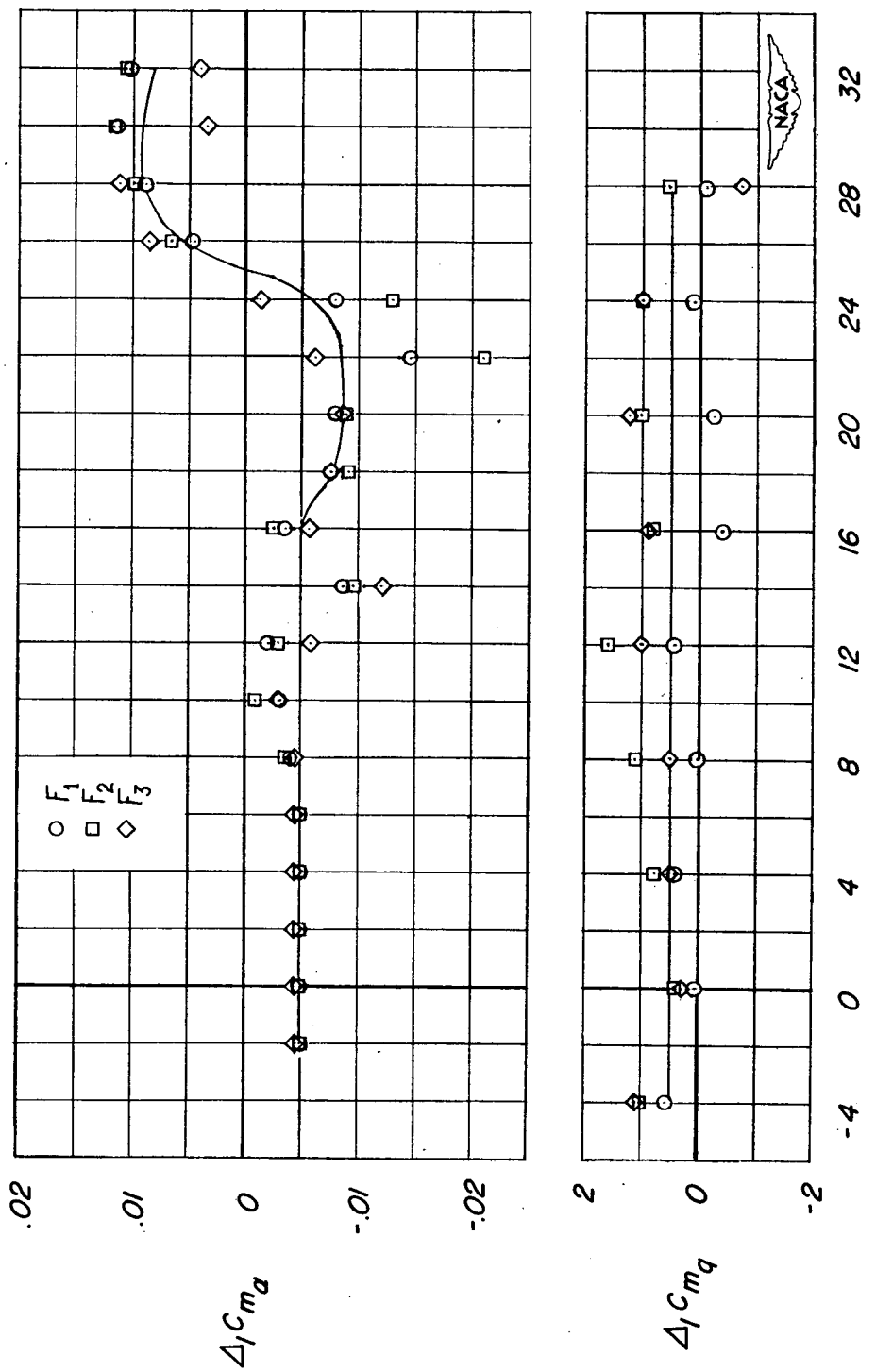

Figure 11.- Variation of wing-fuselage interference increments $\Delta_1 C_{m_\alpha}$ and $\Delta_1 C_{m_q}$ with angle of attack.

NACA TN 2382

National Advisory Committee for Aeronautics.
EFFECT OF HORIZONTAL-TAIL SIZE AND TAIL LENGTH ON LOW-SPEED STATIC LONGITUDINAL STABILITY AND DAMPING IN PITCH OF A MODEL HAVING 45° SWEPTBACK WING AND TAIL SURFACES. Jacob H. Lichtenstein. June 1951. 32p. diagrs., photo., 3 tabs. (NACA TN 2382)

Wind-tunnel results of the effects of horizontal-tail size and length on the low-speed static longitudinal stability and the steady-state rotary damping in pitch for a complete model with wing and tail surfaces having the quarter-chord lines swept back 45° and aspect ratios of 4 are presented.

Copies obtainable from NACA, Washington

1. Wings, Complete - Sweep (1.2.2.2.3)
2. Tail-Wing-Fuselage Combinations - Airplanes (1.7.1.1.3)
3. Stability, Longitudinal - Static (1.8.1.1.1)
4. Stability, Longitudinal - Dynamic (1.8.1.2.1)
5. Damping Derivatives - Stability (1.8.1.2.3)

I. Lichtenstein, Jacob H.
II. NACA TN 2382

NACA TN 2382

National Advisory Committee for Aeronautics.
EFFECT OF HORIZONTAL-TAIL SIZE AND TAIL LENGTH ON LOW-SPEED STATIC LONGITUDINAL STABILITY AND DAMPING IN PITCH OF A MODEL HAVING 45° SWEPTBACK WING AND TAIL SURFACES. Jacob H. Lichtenstein. June 1951. 32p. diagrs., photo., 3 tabs. (NACA TN 2382)

Wind-tunnel results of the effects of horizontal-tail size and length on the low-speed static longitudinal stability and the steady-state rotary damping in pitch for a complete model with wing and tail surfaces having the quarter-chord lines swept back 45° and aspect ratios of 4 are presented.

Copies obtainable from NACA, Washington

1. Wings, Complete - Sweep (1.2.2.2.3)
2. Tail-Wing-Fuselage Combinations - Airplanes (1.7.1.1.3)
3. Stability, Longitudinal - Static (1.8.1.1.1)
4. Stability, Longitudinal - Dynamic (1.8.1.2.1)
5. Damping Derivatives - Stability (1.8.1.2.3)

I. Lichtenstein, Jacob H.
II. NACA TN 2382

NACA TN 2382

National Advisory Committee for Aeronautics.
EFFECT OF HORIZONTAL-TAIL SIZE AND TAIL LENGTH ON LOW-SPEED STATIC LONGITUDINAL STABILITY AND DAMPING IN PITCH OF A MODEL HAVING 45° SWEPTBACK WING AND TAIL SURFACES. Jacob H. Lichtenstein. June 1951. 32p. diagrs., photo., 3 tabs. (NACA TN 2382)

Wind-tunnel results of the effects of horizontal-tail size and length on the low-speed static longitudinal stability and the steady-state rotary damping in pitch for a complete model with wing and tail surfaces having the quarter-chord lines swept back 45° and aspect ratios of 4 are presented.

Copies obtainable from NACA, Washington

1. Wings, Complete - Sweep (1.2.2.2.3)
2. Tail-Wing-Fuselage Combinations - Airplanes (1.7.1.1.3)
3. Stability, Longitudinal - Static (1.8.1.1.1)
4. Stability, Longitudinal - Dynamic (1.8.1.2.1)
5. Damping Derivatives - Stability (1.8.1.2.3)

I. Lichtenstein, Jacob H.
II. NACA TN 2382

NACA TN 2382

National Advisory Committee for Aeronautics.
EFFECT OF HORIZONTAL-TAIL SIZE AND TAIL LENGTH ON LOW-SPEED STATIC LONGITUDINAL STABILITY AND DAMPING IN PITCH OF A MODEL HAVING 45° SWEPTBACK WING AND TAIL SURFACES. Jacob H. Lichtenstein. June 1951. 32p. diagrs., photo., 3 tabs. (NACA TN 2382)

Wind-tunnel results of the effects of horizontal-tail size and length on the low-speed static longitudinal stability and the steady-state rotary damping in pitch for a complete model with wing and tail surfaces having the quarter-chord lines swept back 45° and aspect ratios of 4 are presented.

Copies obtainable from NACA, Washington

1. Wings, Complete - Sweep (1.2.2.2.3)
2. Tail-Wing-Fuselage Combinations - Airplanes (1.7.1.1.3)
3. Stability, Longitudinal - Static (1.8.1.1.1)
4. Stability, Longitudinal - Dynamic (1.8.1.2.1)
5. Damping Derivatives - Stability (1.8.1.2.3)

I. Lichtenstein, Jacob H.
II. NACA TN 2382